


RNF128 expression in lung adenocarcinoma is a favorable prognostic factor associated with decreased tumor-associated macrophages

Syuusuke Fujimoto¹  | Kadota Kyuichi² | Yamada Kaede¹ | Yoshida Chihiro³ | Ibuki Emi⁴ | Ishikawa Ryo⁴ | Haba Reiji⁴ | Yajima Toshiki¹ | Hiroyasu Yokomise¹

¹Thoracic Surgery, Kagawa University, Takamatsu, Japan

²Diagnostic Pathology, Shimane University, Matsue, Japan

³Thoracic Surgery, Kochi Health Sciences Center, Kochi, Japan

⁴Diagnostic Pathology, Kagawa University, Takamatsu, Japan

Correspondence

Kadota Kyuichi, Diagnostic Pathology, Shimane University, Matsue, Shimane, 690-0823, Japan.
Email: kadotak@med.shimane-u.ac.jp

Funding information

SPS KAKENHI, Grant/Award Number: JP20K07392

Abstract

Objectives: Molecular-level research has linked RING finger (RNF) protein family members to carcinogenesis and tumor progression. Among them, RNF128 is related to tumor progression, but reports on its association with lung cancer are few. This study aimed to clarify the unknown association between RNF128 expression and clinical outcomes in patients with lung adenocarcinoma.

Methods: Clinical data of 545 patients with therapy-naïve lung adenocarcinoma who underwent lobectomy with systematic lymph node dissection between 1999 and 2016 were retrospectively reviewed. Histological and immunohistochemical analyses were conducted to evaluate the relationship between RNF128 expression and prognosis.

Results: Among adenocarcinoma histologic types, acinar, micropapillary, and solid tumors did not express RNF128 compared with other histologic types ($p < 0.001$). Patients with high RNF128 expression exhibited fewer clusters of differentiated (CD) 68+ tumor-associated macrophages (TAMs) and CD163+ TAMs. Multivariate analysis of relapse-free survival (RFS) and overall survival (OS) revealed that the lack of RNF128 expression was an independent prognostic factor for poor RFS (hazard ratio [HR] 1.60, $p = 0.029$) and OS (HR 1.83, $p = 0.041$), suggesting that RNF128 expression is a favorable prognostic factor.

Conclusion: RNF128 expression may be an independent predictor of favorable outcomes in Japanese patients with untreated lung adenocarcinoma who undergo surgical resection. Further elucidation of the role of TAM-related E3 ubiquitin ligase in immune function may facilitate the development of effective immunomodulatory therapies for lung adenocarcinoma.

KEYWORDS

carcinogenesis, immunotherapy, lung adenocarcinoma, tumor-associated macrophages

INTRODUCTION

Lung cancer is the most commonly diagnosed cancer and the most common cause of cancer-related deaths worldwide. It can be divided into small-cell lung cancer and non-small-cell lung cancer.¹ Traditional treatment methods, targeted therapies, and immunotherapies have improved therapeutic efficacy rates for patients with lung adenocarcinoma.^{2,3} However, some patients

do not benefit from these treatments. Drug resistance in lung adenocarcinoma treatment also contributes to treatment difficulty,⁴ therefore future molecular-level research into the occurrence and development of lung adenocarcinoma could substantially improve the efficacy of clinical treatments.⁵

The ubiquitin-proteasome system plays a pivotal role in post-translational modifications of proteins and modulates

physiological and pathological processes in eukaryotes. E3 ubiquitin ligases are the core components of this system owing to their specific recognition of substrates.^{6,7} The RING finger (RNF) protein family is a complex set of E3 ubiquitin ligases with an RNF domain. Recently, RNF protein family members have been implicated in carcinogenesis and tumor progression.⁸

RNF128, a gene related to anergy in lymphocytes (GRAIL), is an RNF protein family E3 ubiquitin ligase that participates in T-cell anergy induction.^{9,10} RNF128 deficiency promotes antitumor immune responses from the cluster of differentiation (CD)8+ T cells.¹¹ Moreover, RNF128 interacts with p53 and activates the EGFR/MAPK/MMP-2 pathway, promoting the invasiveness and migratory ability of esophageal squamous cell carcinoma.¹² In melanoma, however, RNF128 regulates Wnt/ β -catenin signaling to suppress epithelial-mesenchymal transformation (EMT) and stemness through a mechanism involving CD44 ubiquitination.¹³ The downregulation of RNF128 expression is associated with poor prognosis in the upper urinary tract and bladder cancers.¹⁴ The low expression of GRAIL in lung adenocarcinoma cells *in vitro* has been associated with poor prognosis,¹⁵ research into the role of RNF128 in lung adenocarcinoma is lacking. The suggested association of RNF128 with EMT and immune antibodies indicates that lung cancer and RNF128 may be related to tumors via similar pathways.

This study aimed to clarify the unknown association between RNF128 expression and clinical outcomes in patients with lung adenocarcinoma. It analyzed a uniform cohort of Japanese patients with therapy-naïve, surgically resected lung adenocarcinoma and investigated whether RNF128 is associated with clinical outcomes and the pathways that affect lung cancer.

METHODS

Patients

This study was conducted in accordance with the Declaration of Helsinki (revised in 2013). The Institutional Review Board of Kagawa University approved the study (approval no. HEISEI 28-030), and the need to obtain individual consent for this retrospective analysis was waived. We reviewed the data of 545 patients with therapy-naïve lung adenocarcinoma who underwent lobectomy or greater resection with systematic lymph node dissection at Kagawa University between 1999 and 2016. Patients with multifocal invasive carcinoma or stage IIb-IV disease were excluded from the study.

Clinical data were collected from a prospectively maintained lung carcinoma database. Disease recurrence was confirmed using clinical, radiological, or pathological assessments. TNM disease stage was assigned based on the 8th edition of the American Joint Committee on Cancer TNM Staging Manual.¹⁶

Histological evaluation

Two pathologists who did not know the clinical outcomes of patients reviewed hematoxylin and eosin (H&E)-stained slides using a BX53 upright microscope (SCR 022568; Olympus Corporation) with a standard 22-mm diameter eyepiece. The tumors were classified according to the 5th edition World Health Organization classification of lung carcinomas. Lymphatic and vascular invasions were noted if at least one tumor cell cluster was visible.

Immunohistochemistry using tissue microarrays

Formalin-fixed, paraffin-embedded tumor specimens from patients who met the inclusion criteria were used for tissue microarray construction. We marked one representative tumor area on the H&E-stained slides. We arrayed a cylindrical 3-mm tissue core from the corresponding paraffin block into a recipient block using an automated tissue processor (Tissue Microprocessor KIN-2; Azumaya). In total, 545 patients had adequate cores available for immunohistochemical analysis.

Subsequently, we obtained 4- μ m sections from tissue microarray blocks and stained them with anti-RNF128 (clone poly, 1:100; Abcam), anti-CD3 antibody (clone 2GV6, prediluted; Ventana Medical Systems), anti-CD4 antibody (clone SP35, prediluted; Ventana Medical Systems), anti-CD45RO antibody (clone UCHL1, 1:200; Leica), anti-CD25 antibody (clone 4C9, prediluted; Nichirei), anti-CD68 antibody (clone KP1, 1:50; Dako), anti-CD163 antibody (clone MRQ-26, prediluted; Cell Marque), E-cadherin (clone NCH-38, prediluted; Dako), and vimentin (clone V9, 1:200; Dako) using a BenchMark ULTRA automated immunohistochemical slide staining system (Ventana Medical Systems) in accordance with the manufacturer's guidelines. Diaminobenzidine was used as the chromogen, whereas hematoxylin was used as the nuclear counterstain. The positive control tissues were stained alongside the study samples.

Immunohistochemical analysis and scoring of immune markers

For immunohistochemically stained slides, the three tumor areas with the highest density of immune cell infiltration, designated as hot spots, were photographed using the BX53 microscope equipped with a DP22 digital camera (Olympus Corporation) under a 20 \times objective lens.

Immune cells for CD3, CD25, CD45RO, and FoxP3 markers were counted on each of the three photographs using the pathoscope image analysis software (version 1.3.0; Mitani Corporation). Immune cells for CD4, CD68, and CD163 markers were manually counted in each of the three photographs via eye-estimation. The average count of the three areas was considered the score for each patient. Based on the expression status of E-cadherin and vimentin,

tumors were classified into three discrete EMT settings as follows: (1) epithelial phenotype – positive for E-cadherin and negative for vimentin; (2) intermediate phenotype – positive for E-cadherin and vimentin, or negative for E-cadherin and vimentin; and (3) mesenchymal phenotype – negative for E-cadherin and positive for vimentin.^{17–19}

RNF128 staining indicated low expression if the percentage of positive tumor cells was less than or equal to the median and high expression if the percentage of positive tumor cells was greater than the median. The intensity of RNF128 staining was not analyzed because no clear distinction in staining intensity was identified among the positive cases (Figures 1 and 2).

Statistical analysis

Associations between variables were analyzed using the chi-square test for categorical variables and the Mann–Whitney U test for continuous variables. Multivariate analysis was conducted using linear regression analysis to evaluate the independent associations of spread through air spaces (STAS) and clinicopathological factors with immune cell

infiltration. Relapse-free survival (RFS) was the time between surgical resection and disease recurrence. Overall survival (OS) was the time between surgical resection and death or the last follow-up date. RFS and OS were estimated using the Kaplan–Meier method, whereas nonparametric group comparisons were performed using log-rank tests. Multivariate analyses were performed using a Cox proportional hazards regression model. Multivariate models were built to include factors identified as significant in the univariate analyses. Associations between pathological factors were examined, and when strong associations were discovered, only one factor was included in the model. All statistical tests were two-sided, with a significance level of 5%. Statistical analyses were conducted using IBM SPSS Statistics for Windows (version 23.0; IBM Corporation).

RESULTS

Clinicopathological characteristics of patients

The median age of the 545 patients was 69 years (range 26–91 years) and more than half were men ($n = 283$, 52%).

FIGURE 1 RNF128 expression in lung adenocarcinoma. (a) Low expression of RNF128. (b) High expression of RNF128

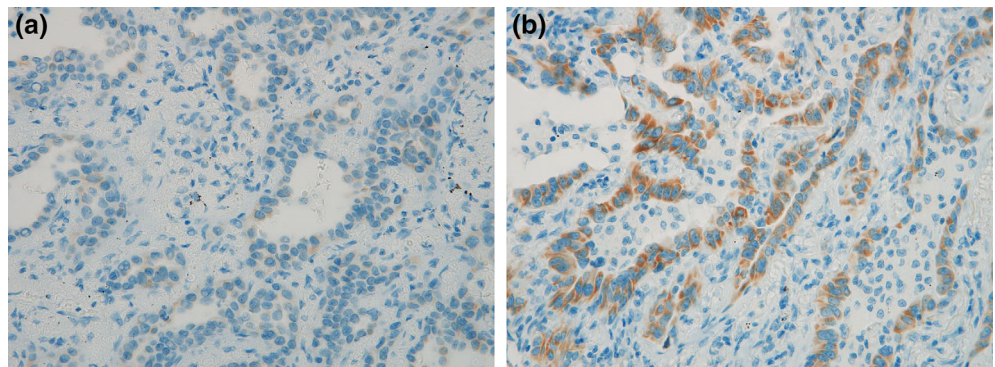
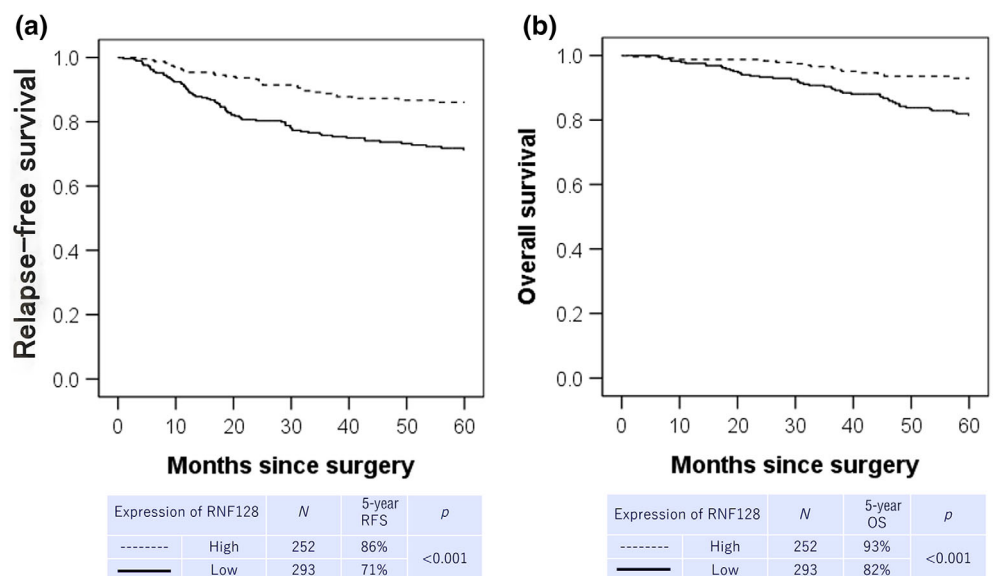


FIGURE 2 Associations between RNF128 expression and relapse-free survival (RFS) and overall survival (OS). (a) Association between RFS and RNF128 expression. Five-year RFS was lower for patients with low RNF128 expression (71%) than those with high RNF128 expression (86%, $p < 0.001$). (b) Association between OS and RNF128 expression. Five-year OS was lower for patients with low RNF128 expression (81%) than those with high RNF128 expression (92%, $p < 0.001$).



Most patients ($n = 407$, 75%) had pathological stage I disease. Of these, 89 (16%) patients received induction therapy. The surgical margins were negative in all cases. In total, 95 patients (17%) received adjuvant therapy. During the study period, 109 patients (20%) experienced recurrence and 63 (12%) died. The median follow-up period for patients who were alive at their last follow-up was 61 months.

Associations of RNF128 with clinicopathological features

The percentage of tumor cells with RNF128 expression was $26 \pm 23\%$ (median 20%, range 0–90%) and 293 patients (54%) had low RNF128 expression with high T stage ($p = 0.008$), higher pathology ($p = 0.032$), lymphovascular invasion ($p < 0.001$), and STAS ($p < 0.001$). When tumors with adenocarcinoma histology were classified based on the predominant subtype, RNF128 was less frequent in the acinar, micropapillary, and solid patterns of adenocarcinoma than in the AIS + MIA, papillary, and lepidic patterns ($p < 0.001$) (Table 1).

Associations of RNF128 with EMT marker and immune cell infiltration

RNF128 expression was not associated with the EMT phenotype (Table 1). Table 2 summarizes the association between RNF128 expression and each type of immune cell infiltration. In patients with RNF128 expression, the number of CD68+ tumor-associated macrophages (TAMs) and CD163+ TAMs reduced slightly, with a significant decreasing trend ($p = 0.01$ each).

Association between patient outcomes and RNF128

Table 3 presents the univariate associations of patient outcomes (RFS and OS) with clinicopathological factors and RNF128 expression. Higher T stage ($p < 0.001$), lymph node metastasis ($p < 0.001$), pathological stage ($p < 0.001$), lymphovascular invasion ($p < 0.001$), and STAS ($p < 0.001$) were significantly associated with a lower RFS. Male sex ($p = 0.016$), higher T stage ($p < 0.001$), lymph node metastasis ($p < 0.001$), pathological stage ($p < 0.001$), lymphovascular invasion ($p < 0.001$), and STAS ($p < 0.001$) were significantly associated with a worse OS.

The 5-year RFS was significantly lower in patients with low RNF128 expression (71%) than in those with high RNF128 expression (86%, $p < 0.001$) (Figure 2a). The 5-year OS was significantly worse in patients with low RNF128 expression (82%) than in those with high RNF128 expression (93%, $p < 0.001$) (Figure 2b).

Multivariate analysis for RFS revealed that low RNF128 expression was an independent prognostic factor for poor

RFS after adjusting for pathological stage and STAS (hazard ratio [HR] 1.60, $p = 0.029$). Multivariate analysis of OS after adjusting for sex, pathological stage, and STAS identified low RNF128 expression as an independent prognostic factor for poor OS (HR 1.83, $p = 0.041$) (Table 4).

DISCUSSION

In this study, we performed immunohistochemical analyses to detect RNF128 expression in lung adenocarcinoma and evaluate its relationship with prognosis. Hence, we examined a large, uniform cohort of patients with therapy-naïve lung adenocarcinoma who underwent lobectomy with systematic lymph node dissection at a single institution. Our findings suggest that RNF128 expression is an independent predictor of good prognosis and is correlated with malignant phenotypes such as tumor size, pathologic stage, the histologic subtype of micropapillary, solid patterns of adenocarcinoma, lymphovascular invasion, and STAS. RNF128, a member of the E3 ubiquitin ligases, is a type I transmembrane protein located in the endosomal compartment.^{20–22} Ubiquitination is a reversible protein post-translational modification that regulates various key biological processes. Ubiquitin is attached to substrates through a catalytic cascade coordinated by multiple enzymes, including E3 ubiquitin ligases.²³ Recent studies have reported that E3 ubiquitin ligases are involved in the progression of various cancers, including esophageal cancer,¹² melanoma,¹³ urothelial carcinomas,¹⁴ and lymphoma.¹¹ A previous study revealed that E3 ubiquitin ligases downregulated RNF128-activated Wnt signaling to induce cellular EMT and stemness via ubiquitinating and degrading CD44/CTTN in melanoma.¹³ However, our study revealed that RNF128 expression was unrelated to EMT.

Several E3 ubiquitin ligases participate in activating and deactivating immune cells in the tumor microenvironment. TAMs are the major components of the tumor microenvironment. TAMs, particularly those with the M2 phenotype, release various growth factors, cytokines, and proteinases that create a favorable microenvironment for tumor progression, resulting in tumor cell dissemination and metastasis.^{24,25} These associations have led to the hypothesis that TAMs may be correlated with RNF128 expression in lung adenocarcinoma.

In this study, we discovered that high RNF128 expression is associated with decreased CD68+ and CD163+ TAMs. One important process influenced by E3 ligases is the polarization of TAMs to the M2 phenotype, creating a protumor microenvironment.^{26,27} TAMs can differentiate into two distinct phenotypes when stimulated by different signals. One is the “classically activated” M1, characterized by CD68 expression, which exerts antitumor effects and secretes pro-inflammatory cytokines such as interleukin (IL)-1, IL-12, IL-23, and tumor necrosis factor- α . M1 polarization results from Th1 cytokine stimulation. The other

TABLE 1 Patient clinicopathological characteristics and their associations with RNF128

Variables		RNF128, n (%)		p
		Low expression	High expression	
Age, years	≤65	103 (52)	97 (48)	0.47
	>65	190 (55)	155 (45)	
Sex	Female	138 (53)	124 (47)	0.69
	Male	155 (55)	128 (45)	
T status	Tis	6 (38)	10 (62)	0.008
	T1	184 (49)	188 (51)	
	T2	80 (67)	40 (33)	
	T3	13 (59)	9 (41)	
	T4	10 (67)	5 (33)	
N status	N0	236 (52)	219 (48)	0.071
	N1	22 (56)	17 (44)	
	N2	35 (69)	16 (31)	
Pathological stage	Stage 0	6 (38)	10 (62)	0.032
	Stage I	208 (51)	199 (49)	
	Stage II	32 (64)	18 (36)	
	Stage III	47 (65)	25 (35)	
Lymphovascular invasion	Absent	151 (47)	169 (53)	< 0.001
	Present	142 (66)	83 (34)	
STAS	Absent	148 (45)	181 (55)	< 0.001
	Present	145 (67)	71 (33)	
EMT-phenotype	Epithelial	144 (55)	116 (45)	0.75*
	Intermediate	128 (52)	118 (48)	
	Mesenchymal	21 (54)	18 (46)	
Histological subtype	AIS + MIA	35 (43)	47 (57)	< 0.001
	Lepidic	30 (40)	45 (60)	
	Acinar	39 (64)	22 (36)	
	Papillary	111 (52)	103 (48)	
	Solid	34 (67)	17 (33)	
	Micropapillary	14 (74)	5 (26)	
	Other	30 (70)	13 (30)	

Note: Significant *p* values are shown in bold.

Abbreviations: AIS, adenocarcinoma in situ; EMT, epithelial mesenchymal transition; MIA, minimally invasive adenocarcinoma; RNF128, RING finger protein 128; STAS, spread through air spaces.

**p* value for epithelial type vs. nonepithelial (intermediate and mesenchymal) type.

TABLE 2 Associations between RNF128 and immune cell infiltration

Marker	Immune cell count, median (range)				p
	RNF128, low expression		RNF128, high expression		
CD3	468	(0–2454)	532	(4–2226)	0.31
CD4	127	(0–683)	137	(10–487)	0.10
CD45RO	253	(5–2058)	298	(21–1600)	0.25
CD25	32	(5–228)	37	(5–475)	0.14
CD68	16	(0–187)	12	(0–187)	0.001
CD163	18	(0–220)	15	(0–197)	0.021

phenotype is the “alternatively activated” M2, characterized by CD68 and CD163 expression, which shows effects opposing those of M1 and mainly secretes anti-inflammatory

cytokines, including IL-4, IL-10, prostaglandin E2, and transforming growth factor- β on activation by Th2 cytokines.^{27,28}

TABLE 3 Univariate associations of patient outcome with clinicopathological factors and RNF128

Variables		n	5-year RFS	<i>p</i>	5-year OS	<i>p</i>
Age, years	≤65	200	74%	0.12	88%	0.27
	>65	345	81%		85%	
Sex	Female	262	78%	0.77	90%	0.016
	Male	283	78%		82%	
T status	Tis	16	100%	<0.001	100%	<0.001
	T1	372	87%		92%	
	T2	120	55%		70%	
	T3	22	58%		71%	
	T4	15	36%		77%	
N status	N0	455	86%	<0.001	81%	<0.001
	N1	39	54%		50%	
	N2	51	24%		46%	
Pathological stage	Stage 0	16	100%	<0.001	100%	<0.001
	Stage I	407	87%		92%	
	Stage II	50	56%		65%	
	Stage III	72	32%		65%	
Adjuvant therapy	Absent	450	82%	<0.001	84%	<0.001
	Present	95	61%		45%	
Lymphovascular invasion	Absent	320	94%	<0.001	95%	<0.001
	Present	225	55%		72%	
STAS	Absent	329	93%	<0.001	96%	<0.001
	Present	216	56%		72%	
Histological subtype	AIS + MIA	82	100%	<0.001	98%	<0.001
	Lepidic	75	94%		96%	
	Acinar	61	61%		72%	
	Papillary	214	78%		88%	
	Solid	51	59%		77%	
	Micropapillary	19	37%		61%	
	Other	43	78%		84%	
	Low	293	71%		82%	
	High	252	86%		93%	

Note: Significant *p* values are shown in bold.

Abbreviations: AIS, adenocarcinoma in situ; MIA, minimally invasive adenocarcinoma; OS, overall survival; RFS, relapse-free survival; RNF128, RING finger protein 128; STAS, spread through air spaces.

TABLE 4 Multivariate analysis

Variables		Hazard ratio	95% CI	<i>p</i>
Relapse-free survival				
Pathological stage	Stage II–III vs. stage 0–I	4.14	2.77–6.20	<0.001
STAS	Present vs. absent	4.34	2.64–7.14	<0.001
RNF128	Low vs. high	1.60	1.05–2.42	0.029
Overall survival				
Sex	Male vs. female	1.41	0.84–2.36	0.19
Pathological stage	Stage II–III vs. stage 0–I	2.80	1.65–4.73	<0.001
STAS	Present vs. absent	3.45	1.81–6.55	<0.001
RNF128	Low vs. high	1.83	1.02–3.25	0.041

Note: Significant *p* values are shown in bold.

Abbreviations: CI, confidence interval; STAS, spread through air spaces; RNF128, RING finger protein 128.

We discovered that low RNF128 expression in resected lung adenocarcinomas is associated with high expression of CD68+ and CD163+ TAMs, suggesting that high RNF128 expression is independently associated with favorable prognosis. These findings suggest that RNF128 and E3 ubiquitin ligase inhibit the polarization of TAMs to the M2 phenotype in lung adenocarcinoma and correlate negatively with the proliferation, migration, and invasion of lung adenocarcinoma. Further research is required to delineate the molecular mechanisms underlying E3 ligase activity and inactivity in regulating immune responses.

This study has several limitations. First, a selection bias was inevitable when selecting tumor areas for tissue microarray construction because this study was based on immunocytochemistry using tissue microarrays. We adopted a 3-mm tissue core and evaluated three tumor areas with the highest density of immune cell infiltration in each core to minimize this bias. Second, as immunohistochemical analysis could not confirm the mechanisms underlying E3 ligases and deubiquitinases related to the tumor microenvironment in immune cells, further experiments using cell lines and animal models are warranted.

Our study's findings suggest that RNF128 expression is an independent predictor of a favorable prognosis. High RNF128 expression is associated with better survival and CD68+ and CD163+ TAMs. If these results reflect a biological correlation between RNF128 and TAMs, the immunological function of TAM-related E3 ubiquitin ligase may promote tumor progression in lung adenocarcinoma. These findings provide a foundation for future investigations into immunomodulatory therapies for lung adenocarcinoma.

AUTHOR CONTRIBUTIONS

All authors had full access to the data in the study and take responsibility for the integrity of the data and the accuracy of the data analysis. Conceptualization: K.K. and R.H. Methodology: K.K. and R.H. Investigation: S.F., K.Y., C.Y., E.I., and R.I. Formal analysis: S.F., K.Y., and C.Y. Resources: K.K. and R.H. Writing – original draft: S.F., C.Y., and K.K. Writing – review and editing: S.F., C.Y., and K.K. Visualization: K.K. Supervision: Y.T. and H.Y. Funding acquisition: H.Y.

ACKNOWLEDGMENTS

The authors thank Toru Matsunaga for assisting with pathology slide preparation and staining. This study was partly supported by JSPS KAKENHI [grant number: JP20K07392].

CONFLICT OF INTEREST STATEMENT

All authors have completed the ICMJE uniform disclosure form. The authors declare no conflicts of interest.

ORCID

Syuusuke Fujimoto  <https://orcid.org/0000-0003-2406-2380>

REFERENCES

1. Ferlay J, Parkin DM, Steliarova-Foucher E. Estimates of cancer incidence and mortality in Europe in 2008. *Eur J Cancer*. 2010;46:765–81.
2. Gautschi O, Milia J, Filleron T, Wolf J, Carbone DP, Owen D, et al. Targeting RET in patients with RET-rearranged lung cancers: results from the global, multicenter RET registry. *J Clin Oncol*. 2017;35:1403–10.
3. Wood K, Hensing T, Malik R, Salgia R. Prognostic and predictive value in KRAS in non-small-cell lung cancer: a review. *JAMA Oncol*. 2016;2:805–12.
4. Sacher AG, Gandhi L. Biomarkers for the clinical use of PD-1/PD-L1 inhibitors in non-small-cell lung cancer: a review. *JAMA Oncol*. 2016;2:1217–22.
5. Xu JY, Zhang C, Wang X, Zhai L, Ma Y, Mao Y, et al. Integrative proteomic characterization of human lung adenocarcinoma. *Cell*. 2020;182:245–261.e17.
6. Buetow L, Huang DT. Structural insights into the catalysis and regulation of E3 ubiquitin ligases. *Nat Rev Mol Cell Biol*. 2016;17:626–42.
7. Akimov V, Barrio-Hernandez I, Hansen SVF, Hallenborg P, Pedersen AK, Bekker-Jensen DB, et al. UbiSite approach for comprehensive mapping of lysine and N-terminal ubiquitination sites. *Nat Struct Mol Biol*. 2018;25:631–40.
8. Senft D, Qi J, Ronai ZA. Ubiquitin ligases in oncogenic transformation and cancer therapy. *Nat Rev Cancer*. 2018;18:69–88.
9. Kriegl MA, Rathinam C, Flavell RA. E3 ubiquitin ligase GRAIL controls primary T cell activation and oral tolerance. *Proc Natl Acad Sci U S A*. 2009;106:16770–5.
10. Lineberry N, Su L, Soares L, Fathman CG. The single subunit transmembrane E3 ligase gene related to anergy in lymphocytes (GRAIL) captures and then ubiquitinates transmembrane proteins across the cell membrane. *J Biol Chem*. 2008;283:28497–505.
11. Haymaker C, Yang Y, Wang J, Zou Q, Sahoo A, Alekseev A, et al. Absence of Grail promotes CD8 T cell anti-tumour activity. *Nat Commun*. 2017;8:239.
12. Gao J, Wang Y, Yang J, et al. RNF128 promotes invasion and metastasis via the EGFR/MAPK/MMP-2 pathway in esophageal squamous cell carcinoma. *Cancer*. 2019;11:6.
13. Wei CY, Zhu MX, Yang YW, Zhang PF, Yang X, Peng R, et al. Downregulation of RNF128 activates Wnt/ β -catenin signaling to induce cellular EMT and stemness via CD44 and CTTN ubiquitination in melanoma. *J Hematol Oncol*. 2019;12:21.
14. Lee YY, Wang CT, Huang SK, et al. Downregulation of RNF128 predicts progression and poor prognosis in patients with urothelial carcinoma of the upper tract and urinary bladder. *J Cancer*. 2016;7:2187–96.
15. Zhu Y, Feng YZWWJ. GRAIL inhibits the growth, migration and invasion of lung adenocarcinoma cells by modulating STAT3/C-MYC signaling pathways. *J BUON*. 2021;26:353–8.
16. Amin MB, Edge S, Greene F, et al. *AJCC Cancer Staging Manual*. 8th ed. New York: Springer; 2017. p. 431–56.
17. Ikeda T, Kadota K, Yoshida C, Ishikawa R, Go T, Haba R, et al. The epithelial-mesenchymal transition phenotype is associated with the frequency of tumor spread through air spaces (STAS) and a high risk of recurrence after resection of lung carcinoma. *Lung Cancer*. 2021;153:49–55.
18. Kalluri R, Weinberg RA. The basics of epithelial-mesenchymal transition. *J Clin Invest*. 2009;119:1420–8.
19. Nijkamp MM, Span PN, Hoogsteen IJ, van der Kogel AJ, Kaanders JH, Bussink J. Expression of E-cadherin and vimentin correlates with metastasis formation in head and neck squamous cell carcinoma patients. *Radiother Oncol*. 2011;99:344–8.
20. Anandasabapathy N, Ford GS, Bloom D, Holness C, Paragas V, Seroogy C, et al. GRAIL: an E3 ubiquitin ligase that inhibits cytokine gene transcription is expressed in anergic CD4+ T cells. *Immunity*. 2003;18:535–47.

21. Heissmeyer V, Macián F, Im SH, Varma R, Feske S, Venuprasad K, et al. Calcineurin imposes T cell unresponsiveness through targeted proteolysis of signaling proteins. *Nat Immunol.* 2004;5:255–65.
22. Seroogy CM, Soares L, Ranheim EA, Su L, Holness C, Bloom D, et al. The gene related to anergy in lymphocytes, an E3 ubiquitin ligase, is necessary for anergy induction in CD4 T cells. *J Immunol.* 2004;173:79–85.
23. Shaid S, Brandts CH, Serve H, Dikic I. Ubiquitination and selective autophagy. *Cell Death Differ.* 2013;20:21–30.
24. Sica A, Larghi P, Mancino A, Rubino L, Porta C, Totaro MG, et al. Macrophage polarization in tumour progression. *Semin Cancer Biol.* 2008;18:349–55.
25. Linde N, Casanova-Acebes M, Sosa MS, Mortha A, Rahman A, Farias E, et al. Macrophages orchestrate breast cancer early dissemination and metastasis. *Nat Commun.* 2018;9:21.
26. Liu Q, Aminu B, Roscow O, Zhang W. Targeting the ubiquitin signaling cascade in tumor microenvironment for cancer therapy. *Int J Mol Sci.* 2021;22:791.
27. Petty AJ, Yang Y. Tumor-associated macrophages: implications in cancer immunotherapy. *Immunotherapy.* 2017;9:289–302.
28. Tariq M, Zhang J, Liang G, Ding L, He Q, Yang B. Macrophage polarization: anti-cancer strategies to target tumor associated macrophage in breast cancer. *J Cell Biochem.* 2017;118:2484–501.

How to cite this article: Fujimoto S, Kyuichi K, Kaede Y, Chihiro Y, Emi I, Ryo I, et al. RNF128 expression in lung adenocarcinoma is a favorable prognostic factor associated with decreased tumor-associated macrophages. *Thorac Cancer.* 2023; 14(17):1581–8. <https://doi.org/10.1111/1759-7714.14901>